Research Paper

Effect of Different Irrigating Solutions and Endodontic Sealers on Bond Strength of the Dentin – Post Interface with and without Defects

Felice R. Grassi[1], Carmine Pappalettere[2,5], Mariasevera Di Comite[3], Massimo Corsalini[1], Giorgio Mori[4], Andrea Ballini[1], Vito Crincoli[1], Francesco Pettini[1], Biagio Rapone[1], Antonio Boccaccio[2,6,✉]

1. Department of Dental Sciences and Surgery, Faculty of Medicine and Surgery, University of Bari "Aldo Moro", Bari, Italy
2. Department of Mechanical and Management Engineering, Polytechnic of Bari, Bari, Italy
3. Department of Human Anatomy and Histology, Faculty of Medicine and Surgery, University of Bari "Aldo Moro", Bari, Italy
4. Department of Biomedical Sciences, University of Foggia, Foggia, Italy
5. President of EuraSEM, European Society for Experimental Mechanics
6. Società Cooperativa Sociale e Sanitaria: ONLUS "Insieme con Padre Pio"

✉ Corresponding author: Dr. Antonio Boccaccio. Dipartimento di Ingegneria Meccanica e Gestionale, Politecnico di Bari, Viale Japigia, 182, I-70126, Bari, Italy. Tel: +39-0805962829. Fax: +39-0805962777. E-mail: a.boccaccio@poliba.it

Abstract

Aims. To investigate how the interfacial shear strength of the dentin – post interface with and without defects changes for different combinations irrigant/sealer.

Methods. In forty human decoronated and instrumented teeth, fibreglass posts were inserted. The obtained root segments were randomly assigned to four different groups according to the irrigant adopted and the cement used to seal the root canal. The root segments were processed for metyl-methacrylate embedding. Serial sections were obtained and submitted to histomorphometric analyses in order to observe any defect of adhesion at the dentin – post interface and to measure the defects' dimension. The serial sections were also submitted to micro-push-out test. The measured shear strength values were subjected to statistical analysis by one-way ANOVA. The values of bond strength determined for the defective samples were correlated with the dimension of the defects. Finite element models were built to interpret and corroborate the experimental findings.

Results. ANOVA showed that the generic combination irrigant/sealer does not affect the interfacial shear strength values. The bond strength of the samples without defects was averagely twice as large as that of the defective samples. The defects occupying more than 12 % of the total transverse section area of the endodontic cement layer led to a reduction of the bond strength of about 70 %. The predictions of the finite element models were in agreement with the experimental results.

Conclusion. Defects occupying less than 2 % of the total transverse section area of the cement layer were shown to be acceptable as they have rather negligible effects on the shear strength values. Technologies/protocols should be developed to minimize the number and the size of the defects.

Key words: Defect of Adhesion, Finite Element Method, Histomorphometric Analyses, Interfacial Shear Strength, Micro-Push-Out Test, Microradiography.

Introduction

Fibre posts play a role of crucial importance in the restoration of endodontically treated teeth. Due to their Young's modulus closely matching that of tooth structures, fibre posts showed a reduced risk of failure and more favourable outcomes [1-6] when compared with the traditional metallic posts. They are ready to use and allow the restoration procedure to be conducted in a shorter time [1-3] with relatively low costs [7-9].

The restoration of endodontically treated teeth is guided by two principal requirements: strength and aesthetics. The main objective that must be pursued in the tooth restoration is to transfer the functional load from the coronal and root restoration to the remaining tooth structure [4, 10, 11] with a stress distribution as similar as possible to that of the tooth in the physiological conditions. The quantity and the shape of the remaining coronal and root dentin, the materials utilized, as well as the bonding interaction between the biological tissues and the biomaterials will influence the outcome of the restoration. The Interfacial Shear Strength (ISS) at the Dentin – Post Interface (DPI) has been measured through different mechanical testing methods: microtensile bond strength, pull-out and push-out tests [12]. A modification of the push-out test, by reducing the specimen thickness, is called micro-push-out test and is reported to offer different advantages [12-14].

Many *in vitro* studies have investigated the different factors affecting the interfacial shear strength at the dentin – post interface [15-20]. Some of these factors are represented by the intracanalar irrigant as well as the endodontic cement used to seal the root canal. Chemical irrigants are essential for successful debridement of root canals during shaping and cleaning procedures [21-24]. They are used not only as antimicrobial agents but also to lubricate the dentinal walls and to dissolve organic and inorganic components of the smear layer [25]. Sodium hypochlorite (NaOCl) has long been proved to present capacity of dissolution of organic tissues and neutralization of toxic products while chlorhexidine (CHX), in addition to capacity of dissolution, has also been shown to possess bactericide properties because of its ability to precipitate and coagulate bacterial intracellular constituents [26]. Irrigants might affect the characteristics of the dentin surface and therefore, might trigger or inhibit the chemical (e.g. covalent bonds, metallic bonds, etc), physical (e.g. van der Walls forces, hydrogen bonds, etc) and mechanical (e.g. entrapment of a material into another body, within natural or artificial cavities) attraction forces which are involved in

the process of adhesion of the post to the dentin. In the regions where these forces have a small intensity, defects might originate such as inclusions of gas bubbles. In addition, the residues of endodontic sealer accidentally left on the root canal walls, might originate defects of polymerization within the endodontic cement and this could affect the bond strength of a post to intraradicular dentin. In spite of the huge number of studies on the effects of chemical irrigants and endodontic sealers on the interfacial shear strength, little information is available regarding the effects of defects accidentally included in the cement layer at the DPI. The aim of this study was to investigate (i) how the interfacial shear strength changes for different irrigant/sealer combinations, and (ii) how the presence of defects can affect the ISS. Regarding the objective (i), the shear strength values measured in the micro-push-out test, were subjected to statistical analysis by one-way ANOVA. The null hypothesis was that the combination irrigant/sealer does not affect the values of the interfacial shear strength at the DPI. Concerning the objective (ii), the values of ISS determined for the defective samples were put in correlation with the dimensions of the defects measured through histomorphometric analyses. Finite element models simulating the stress state in the samples with and without defects during the micro-push-out test were finally built to interpret and corroborate the experimental findings.

Materials and Methods

Collection and preparation of samples

Forty human single-rooted teeth were collected and used in the present study. All teeth were extracted for orthodontic reasons and kept, according to Jainaen et al. [27], in 1 % chloramine T (pH 7.8) at 4 °C until use. By using a high speed carbide bur and water spray, the dental crowns were removed obtaining approximately 15 mm long root segments. The obtained roots were then randomly assigned to four groups (*n*=10) according to the irrigating solution used as well as to the type of endodontic cement employed to seal the root canal space. Canal patency and working length were established by inserting K file #15 (DENTSPLY Maillefer, Oklahoma, USA) to the root canal terminus. All canals were prepared at working length 0.5 mm short of the patency length using 0.04 taper Profile instrument (DENTSPLY Maillefer, Oklahoma, USA) to master apical rotary (MAR) size 35–45. In order to remove the smear layer left by every file, the root canals were abundantly

irrigated with chlorhexidine 0.2 % (Group A and D) or sodium hypochlorite 5 % (Group B and C). Canals were dried using paper points. Pulp Canal Sealer™ (EWT KERR®, Orange, CA, USA), cement based on zinc oxide and eugenol, was used for the Group A and B, while Apexit (IVOCLAR VIVADENT®, Naturno (BZ), Italy), cement based on calcium hydroxide, was used for the Group C and D. After mixing the sealer, a gutta-percha master cone was lightly coated with sealer and inserted to the working length. A System B plugger size fine medium was used to condense the master cone to within 5 mm from the working length. Gutta-percha and sealers were removed with Gates-Glidden (DENTSPLY Maillefer, Oklahoma, USA) instruments and a 4÷5 mm thick layer was left on the root canal terminus so to guarantee its sealing. Then, root canals were abundantly irrigated with sodium hypochlorite 5 % (Group B and C), or chlorhexidine 0.2 % (Group A and D); paper points were again used to dry their surface. Fiberglass posts were inserted according to the protocol prescribed by the posts' Manufacturer (MC Italia, Milano, Italy). The choice of the post was made according to the size of the root canal. Using a Surgi Shaper cutter disk, the post was adapted apically. The root canal walls were treated with the Surgi Gel acid solution (phosphoric acid 37 %) for sixty seconds to etch dental tissues and obtain a stronger adhesion. The acid was accurately removed by water spray. Paper points were again used to dry the root canal. However, this time, the dentinal surface was left wet. By using a micro-brush, a first layer of dual adhesive Surgi Primebond Base + Surgi Primebond Activator (MC Italia, Milano, Italy) was applied on the root canal walls. Then, the layer was radiated by a halogen lamp for twenty seconds. A second layer of dual adhesive was applied, but, this time, the adhesive was not radiated (to avoid the formation of an additional thickness that would push the post in the direction of the crown). The dual adhesive was also applied on the post surface. The Surgi Dual Flò Core cement (MC Italia, Milano, Italy) was slowly extruded within the root canal thus filling it completely. The post was finally inserted; the excessive amounts of cement that came out of the root canal were radiated by a halogen lamp for forty seconds to stabilize the emergent part of the post.

All the operations were carried out by a single experienced operator.

Histomorphometric analyses

The teeth with the inserted posts, were fixed in 4 % paraformaldehyde in 0.01 M phosphate-buffered saline solution (PBS pH 7.2) for 2 days at 4°C, well washed in running water for 2 hours, dehydrated in

ethanol and conventionally processed for metyl-methacrylate (that, after polymerization, becomes Poly(metyl-methacrylate) PMMA) embedding. By alternating 70 μm and 1000 μm thick, serial sections were obtained according to a transverse plane (Figure 1) by means of a circular diamond-bladed saw (SP1600 Leica Microsystems, Wetzlar, Germany), polished under running water and air dried in incubator at 37 °C for 24 h. All the 70 and 1000 μm thick sections were coded and microradiographed at 8 kV and 14 mA by using a XRG-3000 x-ray generator (Ital Structures Research, Riva Del Garda, Italy) and a Kodak High Resolution Film. Contact microradiographs were developed in Kodak HC-110, fixed in Ilford Hypam Rapid Fixer, washed in bidistilled water and air dried at room temperature. Histomorphometric analyses by means of a light microscope (Nikon Eclipse E 400) associated to a digital camera (Nikon DS-5M) and an image processing software (Nikon Nis-Elements BR), were carried out on microradiographies. Three different types of defects were identified:

(a) inclusion of gas bubbles within the cement layer;

(b) detachment at the dentin – cement interface;

(c) traces of primary cement (for the sealing of the root canal) into the secondary cement.

The 70 μm thick sections served to better visualize and reconstruct the morphology of the defects of the 1000 μm thick sections immediately adjacent. If A_t and A_d are, respectively, the total area of the surface occupied by the secondary cement and by the defect, the defect percentage area A_{dp} was defined as:

$$A_{dp} = \frac{A_d}{A_t} \times 100$$

…(1)

Measurements of A_{dp} were carried out for every 1000 μm thick sections. The (1000 μm thick) sections for which the histomorphometric analyses revealed the presence of defects were classified as defective.

Micro-push-out test

For each of the collected roots, approximately 5÷6 1000 μm thick sections have been obtained; a total of 220 sections were therefore submitted to micro-push-out-test. The micro-push-out test was performed on a 3343 Instron universal testing machine with a load cell of 500 N. Following Teixeira et al. [17], the crosshead speed was set equal to 1 mm/min. A couple of guides firmly fixed to the grips (controlled by a hydraulic system) of the testing machine, guaranteed the exact vertical positioning of a steel rod (Figures 2a and 2b). The rod had a circular transverse

section; according to Hashem et al. [22], the diameter of the steel rod was set equal to 0.8 mm. The specimens were placed onto an aluminium plate 10 mm thick with a 2 mm diameter circular hole. The plate was fixed, in turn, by means of a supporting frame, to the bottom grips of the testing machine (Figures 2a and 2b). All tested specimens included posts possessing a transverse section with a diameter greater than the rod diameter. For each sample, the force-displacement curve was traced thus distinguishing four different regions. An initial region (highlighted in red, Figure 2c) in which, due to the clearance existing between the sample and the aluminium plate, as well as the rod tip and the sample, small values of force were registered against large displacement values; a second region (highlighted in blue, Figure 2c) where a quasi-linear increase of the force with the displacement was observed; a third region (highlighted in green, Figure 2c) where a sudden decrease of the force was recorded, - which indicates that the critical condition of failure have been reached -; a fourth region (in grey, Figure 2c) where, due to the fact that the portions of the adhesive area at the post – cement interface that did not fail yet opposed the further displacement of the rod, a small increase of the force was observed. The interfacial shear strength was computed as the ratio between the maximum value of force (registered in the third re-

gion) and the bonding area at the dentin – post interface. The bonding area was accurately measured through the histomorphometric images of the 70 μm thick samples immediately adjacent (to the 1000 μm thick section under analysis).

The test was considered not acceptable in each of the following cases:

i) failure of the dentin occurring before the failure of the cement;

ii) failure of the PMMA occurring before the failure of the cement;

iii) failure of the dentin and of the PMMA occurring before the failure of the cement;

iv) penetration of the rod within the post without failure of the cement.

The samples to be tested have been randomly chosen. The experimental results were subjected to statistical analysis by One-Way ANOVA. The null hypothesis H_o was that the generic group (i.e. the combination irrigant/sealer) does not affect the values of the interfacial shear strength at the DPI. H_o was assumed to hold true for *p-values* > 0.05 (i.e. interval of confidence of the 95 %). The values of ISS experimentally determined for the samples with defects were finally put in correlation with the dimensions of the defects observed via histomorphometric analyses.
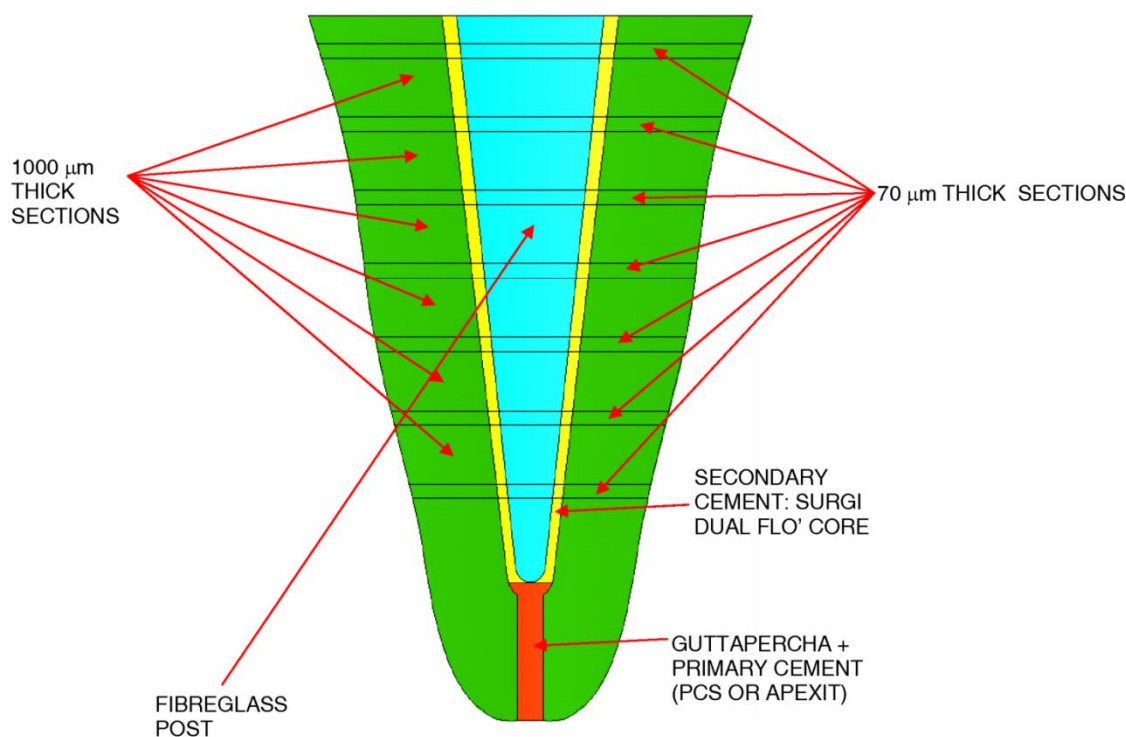
Figure 1. Cutting sequence followed to obtain the slices for histomorphometric analyses and micro-push-out test.
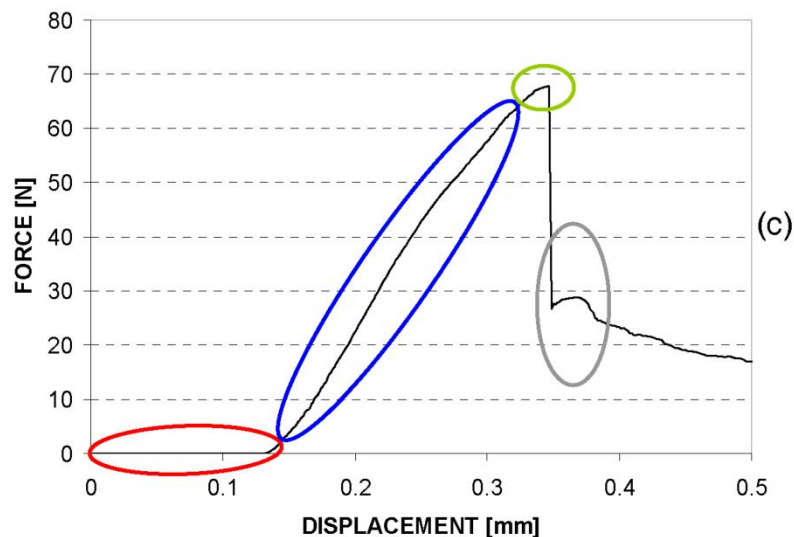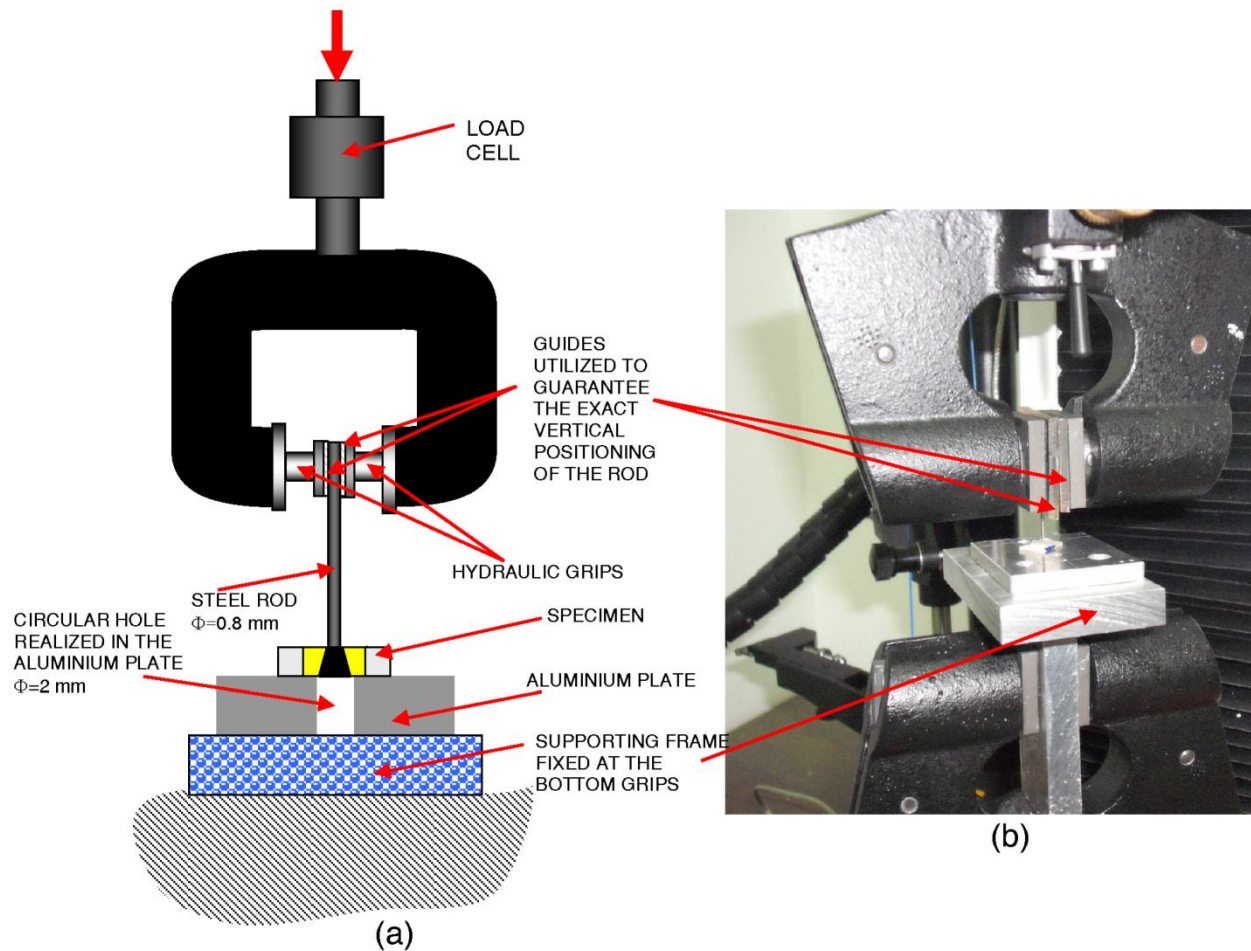
Figure 2. Schematic (a) and picture (b) of the loading system utilized to perform the micro-push-out test; (c) typical force-displacement curve registered for the generic sample submitted to micro-push-out test. Four different regions can be distinguished. An initial region (highlighted in red) in which, due to the clearance existing between the sample and the aluminium plate, as well as the rod tip and the sample, small values of force are registered against large displacement values; a second region (highlighted in blue) where a quasi-linear increase of the force with the displacement occurs; a third region (highlighted in green) where a sudden decrease of the force occurs, which indicates that the critical condition of failure has been reached; a fourth region (highlighted in grey) where, due to the fact that the portions of the bonding area at the post-cement interface that did not fail yet oppose the further displacement of the rod, a small increase of the force is observed.

## Modeling of the micro-push-out-test: Finite Element Analysis

A finite element model was built reproducing the micro-push-out-test (Figure 3). An analytic rigid surface simulated the steel rod pushing against the post. A layer of cement 0.1 mm thick was hypothesized to occupy the space between the post (in blue, Figure 3) and the dentin (in yellow, Figure 3). The taper angle of the post was set equal to 6°. The post, the cement layer, the dentin and the PMMA in which the tooth slice is embedded were modeled as solids of revolution, all with the same revolution axis. Constraints preventing the displacement along the vertical direction have been applied on all the nodes of the lower base of the PMMA model as well as on those of the lower base of the dentin model placed outside a 2 mm (i.e. the diameter of the hole realized in the aluminum plate) diameter circumference. Constraint equations have been used to attach the lateral surface of the post with the internal surface of the cement layer; the same constraint equations have been used at the cement – dentin and the dentin – PMMA interface. A concentrated force of 60 N, was applied on a node of the analytical surface simulating the steel rod. The experimental tests showed that for the samples with dimensions comparable with those utilized in the finite element model, 60 N is a threshold value beyond which the failure of the sample occurs. Four different models have been built to simulate the cement layer located between the post and the dentin: (i) the first one (Figure 4a) simulated a layer of cement without defects; (ii) the second, the third and the fourth one simulated the defects (a) (Figure 4b), (b) (Figure 4c) and (c) (Figure 4d), respectively, described above and observed in the histomorphometric analyses. The dimension of the simulated defects has been set equal to the average dimension of the same defects (see pictures in Figure 4) observed via histomorphometric analyses.
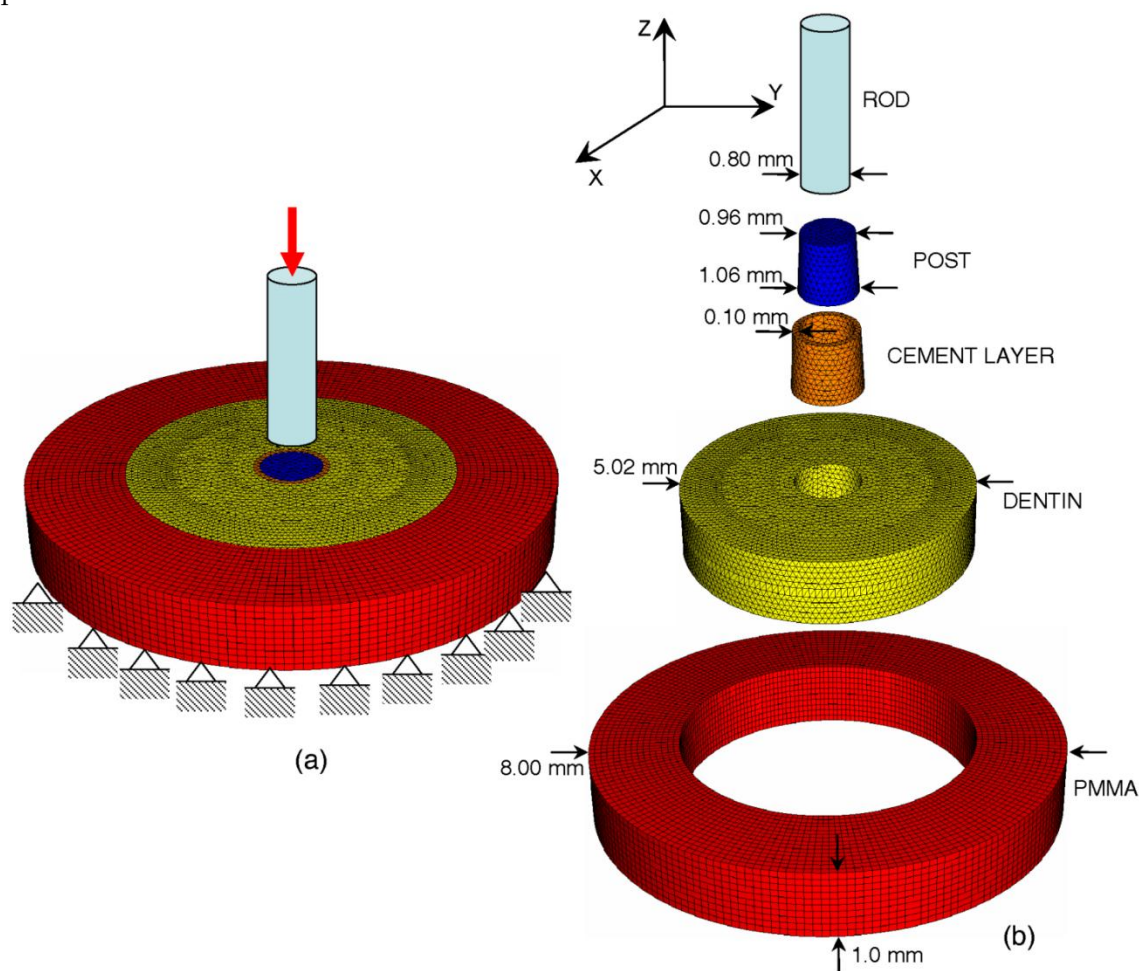
Figure 3. (a) Assembly view of the finite element model utilized to simulate the micro-push-out test; the boundary and loading conditions are also schematized. (b) Details of the different parts included in the finite element model.
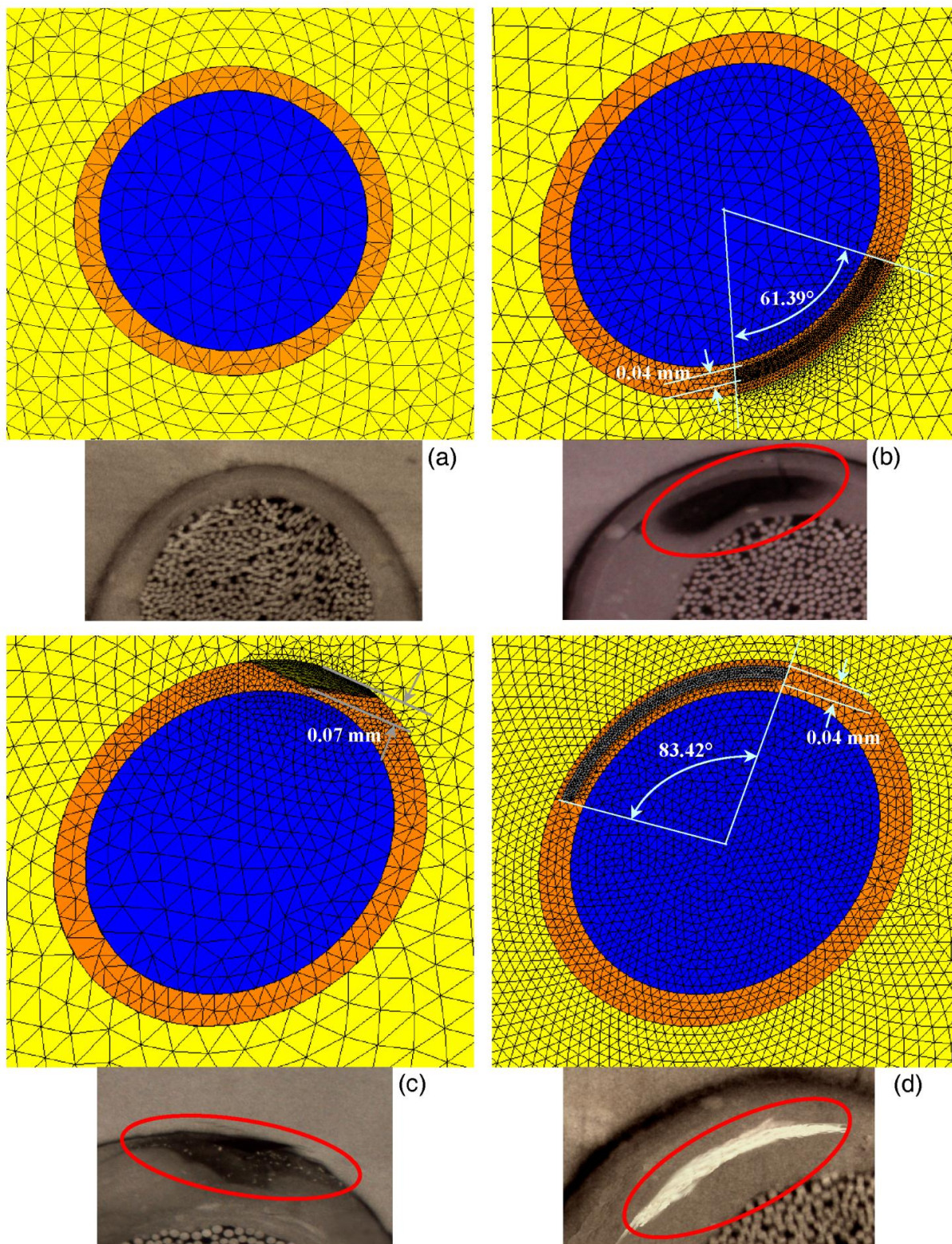
Figure 4. Details of the finite element model of the cement layer at the dentin – post interface in the case of: (a) cement layer without defects; (b) gas bubble included within the cement layer; (c) detachment at the dentin – cement interface; (d) traces of primary cement (for the sealing of the root canal) into the secondary cement. In the pictures are highlighted in red the "average" defects observed in the histomorphometric analyses and reproduced in the finite element models.

The PMMA, the dentin and the cement have been modeled as linear-elastic, homogeneous and isotropic materials. Table 1 lists the values of the mechanical properties utilized in the finite element model. The primary cement was hypothesized to possess a Young's modulus equal to the 10 % of the Young's modulus of the secondary cement. The post was modeled as an orthotropic material (E_{zz}=37 GPa, E_{xx}=9.5 GPa, E_{yy}=9.5 GPa, ν_{yz}=0.27, ν_{xz}=0.34, ν_{xy}=0.27) the principal material directions (shown in Figure 3) and elastic moduli of which have been taken from Soares et al. [12].

The analyses were performed with the general purpose finite element code ABAQUS (Hibbit *et al.*, Dassault Systèmes Simulia Corp., Providence, RI). Four nodes tetrahedral C3D4 elements available in ABAQUS were used to mesh the volume of the dentin, the cement layer and the post. Hexahedral C3D8 elements were instead used to mesh the volume of the PMMA. Four finite element analyses were performed, one for each of the models of the cement layers described above.

Table 1. Material properties utilized in the FEM analyses

MATERIAL	YOUNG'S MODULUS (GPa)	POISSON'S RATIO
PMMA	3.0	0.37
SURGI DUAL FLÒ CORE	15.0[28]	0.27
PRIMARY CEMENT	1.5	0.27
DENTIN	18.6[29]	0.31

Results

The dimension of the defects appeared to be insensitive to the combination irrigant/endodontic sealer (Figure 5b). For each of the investigated groups, the median value, the first quartile, the third quartile, the minimum and the maximum values were indicated (Figure 5a). Also the values of the interfacial shear strength appeared not to depend (Figure 6a) on the group (irrigant/endodontic sealer) in which the samples were classified. Table 2 lists the mean and the standard deviation of the shear strength values measured with the micro-push-out test. One-way Analysis of the Variance (ANOVA) revealed that the null hypothesis H_0 holds true (*p-value*=0.280) which indicates that the interfacial shear strength at the DPI is insensitive to the combination irrigant/endodontic sealer. However, if one separates, for each of the investigated groups, the samples that, at the histomor-

phometric analyses, appeared without defects from those that presented defects, significantly smaller values of standard deviation are determined (Table 3). The values of interfacial shear strength found for the samples without defects were on average twice as large as those found for the defective samples (Table 3 and Figures 6b and 6c). A rather good correlation could be found between the dimension of the defects and the values of shear strength (Figure 7).
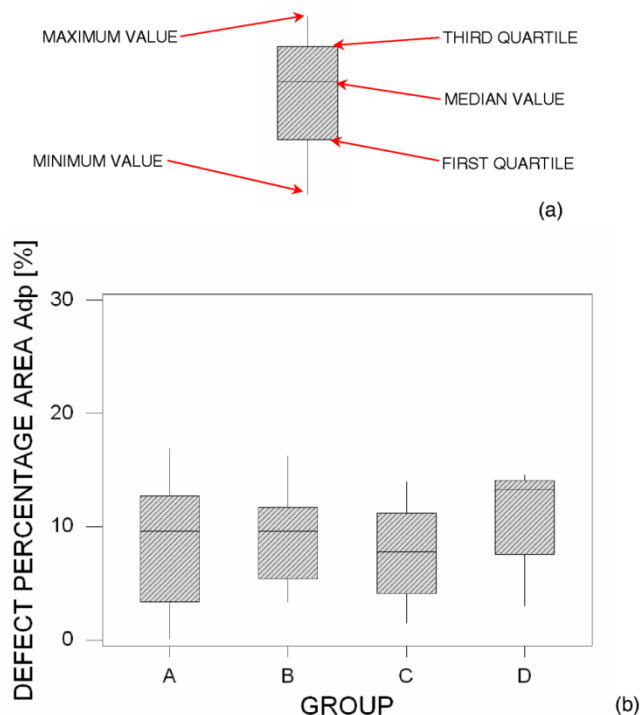
Figure 5. Boxplot of the defect percentage area A_{dp} measured in the histomorphometric analyses (b). For each of the investigated groups, the median value, the first quartile, the third quartile, the minimum and the maximum values are indicated (a).

For a more robust statistical description of the experimental data, the percent variation coefficient (C_v), defined as the ratio between standard deviation and average value, was used. While the standard deviation measures the dispersion of a given set of values, the C_v parameter allows data dispersion to be correlated with the average value of the measured quantity. Therefore, high values of C_v will indicate a large dispersion with respect to the average measure and then low reliability of measurements. Figure 8 shows how the C_v parameter decreases when the samples with defects are excluded from each group.

The normalized values of the von Mises stresses computed with the finite element method were significantly higher (about 2 times) in the case of defects included (Figure 9). Furthermore, while a rather reg-

ular distribution of the von Mises stresses has been computed in the case of samples without defects, local stress peaks were predicted, instead, in the vicinity of the defects for the defective samples.

Table 2. Mean and standard deviation of the interfacial shear strength values measured with the micro-push-out test for each of the investigated groups.

	GROUP A	GROUP B	GROUP C	GROUP D
AVERAGE [MPa]	15.1	14.1	14.0	16.8
STANDARD DEVIATION [MPa]	4.6	4.4	6.0	5.4

**Table 3.** Mean and standard deviation of the interfacial shear strength values measured with the micro-push-out test for each of the investigated groups in the case of samples with and without defects.

|	GROUP A	GROUP B	GROUP C	GROUP D	
AVERAGE [MPa]	17.8	18.4	19.9	20.4	SAMPLES WITHOUT DEFECTS
STANDARD DEVIATION [MPa]	3.4	3.2	2.3	3.3	
AVERAGE [MPa]	11.0	10.7	8.8	12.0	SAMPLES WITH DEFECTS
STANDARD DEVIATION [MPa]	2.0	1.4	1.5	2.4	
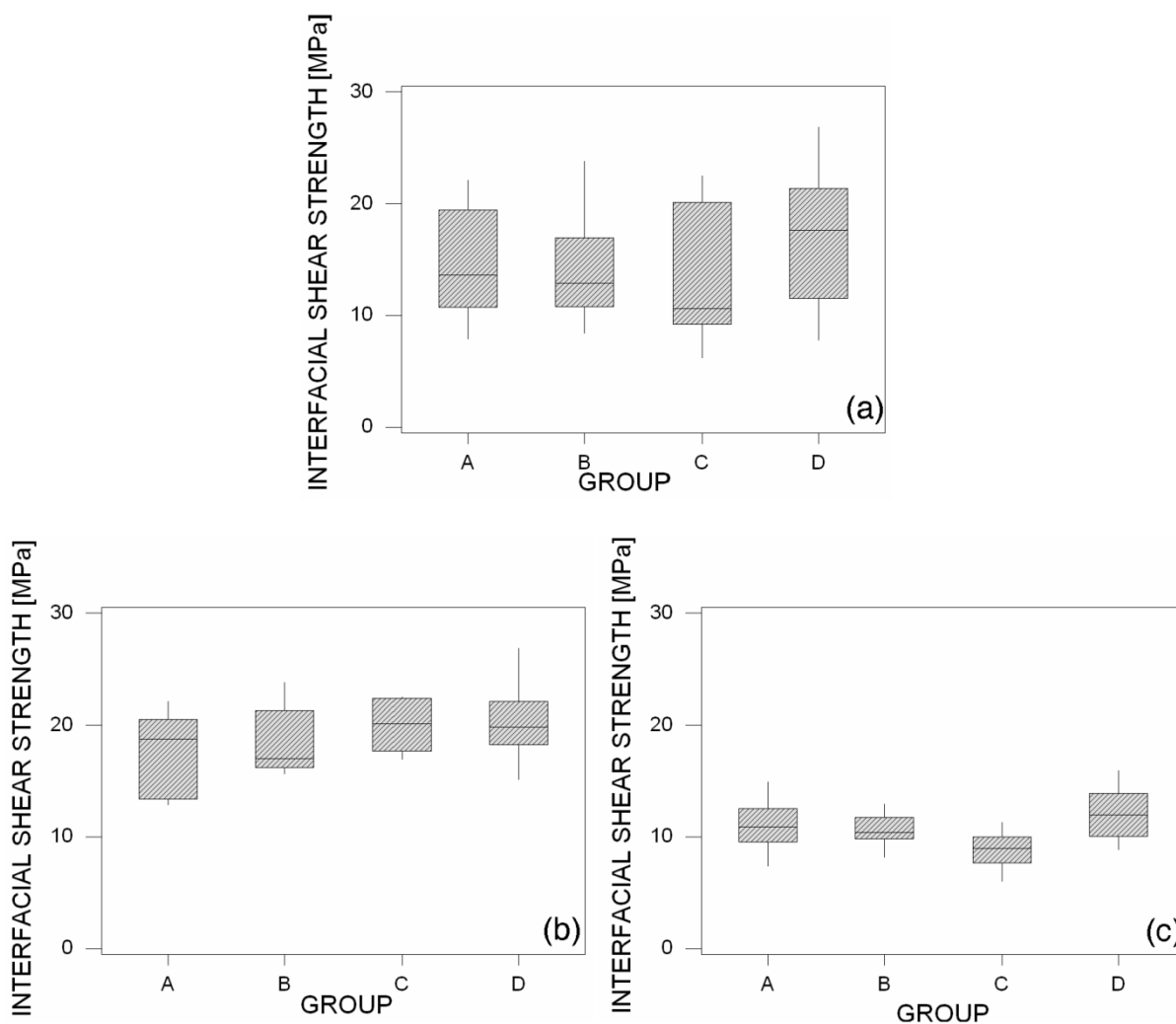
Figure 6. Boxplot of interfacial shear strength measured in the micro-push-out test in the case of samples with and without defects (a), without defects (b) and with defects (c).
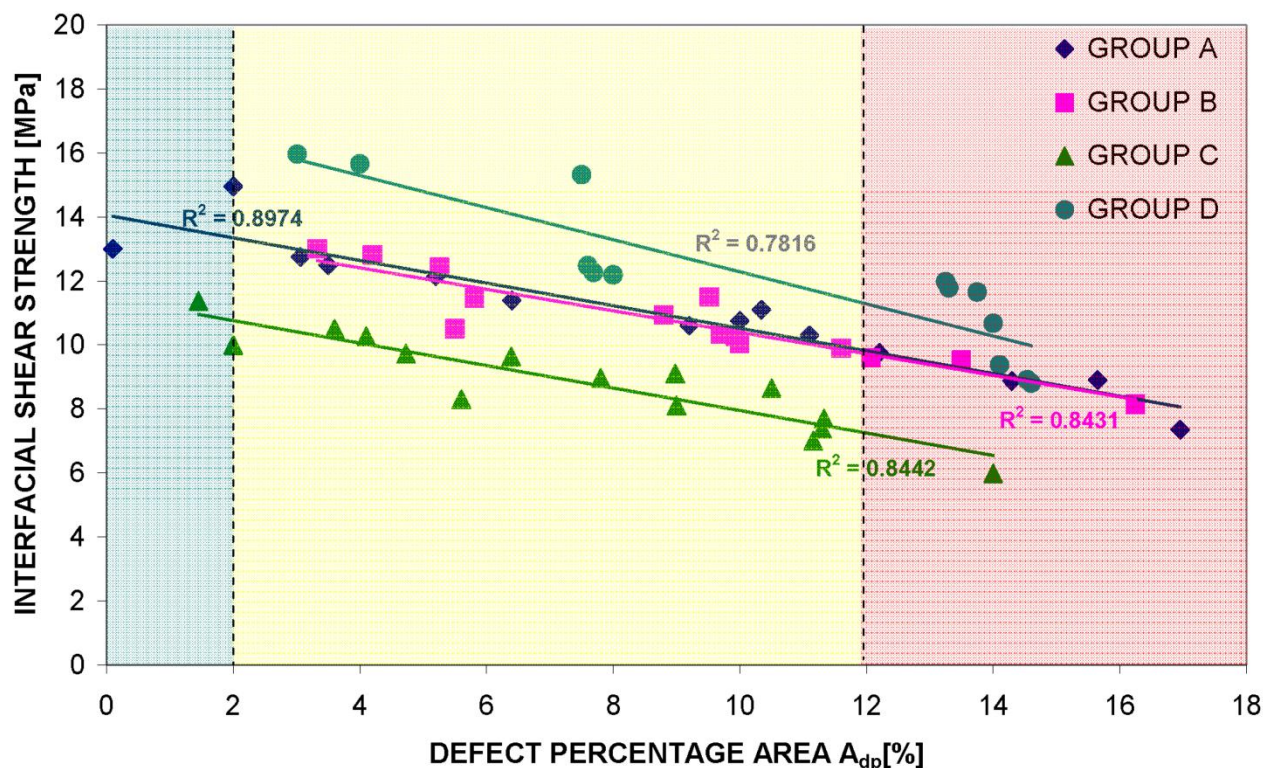
Figure 7. Interfacial shear strength of samples with defects vs. dimension of the defects (i.e. the defect percentage area A_{dp}). Three different regions can be distinguished: a first region (highlighted in blue, with $A_{dp} \leq 2$ %) where the dimension of the defects is rather negligible and the values of interfacial shear strength are comparable with the minimum values of ISS found for the samples without defects; a second region (highlighted in yellow, with 2 % $\leq A_{dp} \leq 12$ %) where the ISS values are significantly smaller than those found for the samples without defects; a third region (highlighted in red, with $A_{dp} \geq 12$ %) where, due the large dimension of the defects, the ISS values are about 70 % smaller than the ISS values found for the samples without defects.
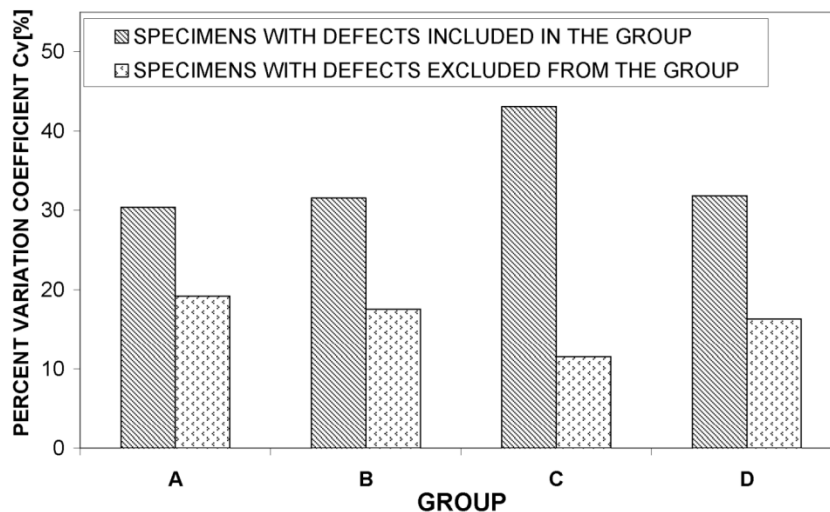
Figure 8. Percent coefficient of variation C_v determined for each of the investigated group in the case of defective specimens included and defective specimens excluded.
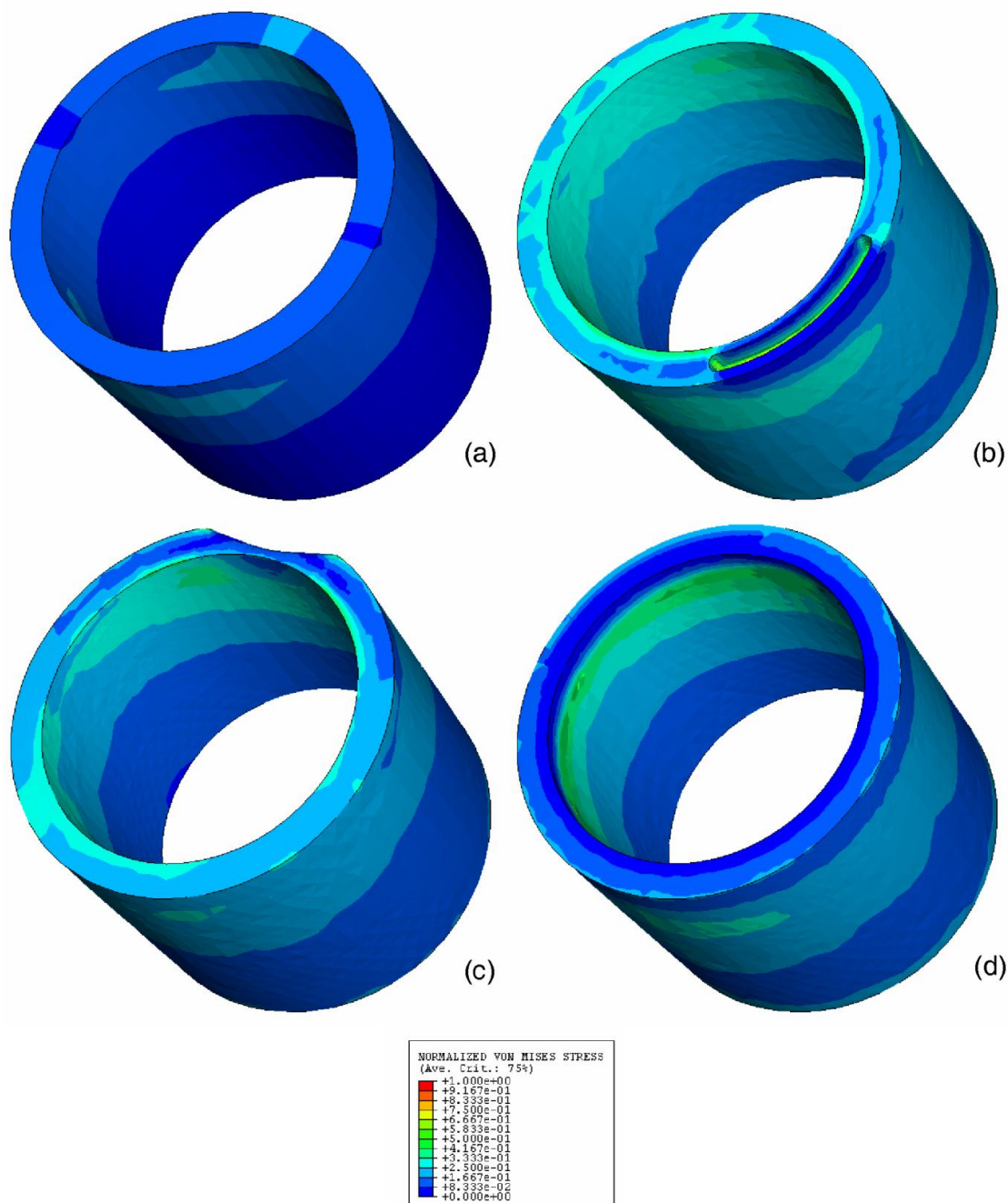
Figure 9. Normalized von Mises stress distribution in the cement layer computed with the finite element method in the case of: (a) cement layer without defects; (b) gas bubble included within the cement layer; (c) detachment at the dentin/cement interface; (d) traces of primary cement included within the secondary cement.

Discussion

In this study, we investigated how the ISS at the dentin – post interface changes for different irrigants and endodontic sealers as well as how the values of the bond strength change in the presence of defects accidentally included in the endodontic cement layer.

The present study has some limitations. In the first place, simplified finite element models of the cement layers with defects have been built. Ideally, a more precise reconstruction of these models requires a micro-CT scanning of the samples and then the generation of the finite element mesh. This approach allows the morphology of the defects to be reproduced with a great deal of details, however, is very expensive in terms of computational cost [30]. Second, linear elastic finite element analyses were performed; the implementation of non-linear elasto-plastic mod-

els would allow the local phenomena of defect plasticization and therefore, the global structural response of the sample to be better reproduced [31]. However, such a modeling approach goes behind the scope of the present article and will be further developed in future studies.

The dimension of the defects was shown to be rather insensitive to the group in which the samples were classified (Figure 5). The high values of standard deviation did not permit to identify one or more combinations irrigant/sealer that allows smaller defects to be obtained. Also the values of ISS appeared not to depend on the generic group (Figure 6a); one-way ANOVA showed that the combination irrigant/sealer does not affect the shear bond strength at the dentin – post interface (*p-value* > 0.05). The interfacial shear strength means as well as the standard deviations experimentally found (Figure 6a) were consistent with those reported in other studies [12]. However, if one separates the samples without defects from those with defects, significantly smaller standard deviations can be obtained (Table 2 and 3, Figures 6 and 8); the ISS values exhibited by the first ones was about twice as large as that exhibited by the second ones (Figure 6). This result was in agreement with the numerical predictions of the finite element models. It was found, in fact, that the maximum von Mises stress values in the models simulating the samples with defects are about twice as large as those found in the model reproducing the sample without defects (Figure 9). In general, the higher von Mises stress values the greater risk of failure of the sample. The smaller values of the standard deviations obtained by excluding the defective samples (Figures 6 and 8) indicated a smaller data distribution variability and therefore, a more reliable test and a more controllable response of the tested samples. Finally, for increasing dimensions of the defects decreasing values of ISS have been measured (Figure 7). Three different regions could be distinguished: a first region (highlighted in blue, with $A_{dp} \leq 2$ %, Figure 7) where the values of shear strength are comparable with the minimum values of ISS found for the samples without defects (Figures 6b and 7); a second region (highlighted in yellow, with 2 % $\leq A_{dp} \leq 12$ %, Figure 7) where the ISS values are significantly smaller than those found for the samples without defects; a third region (highlighted in red, with 12 % $\leq A_{dp}$) where, due the large dimension of the defects, the ISS values are about 70 % smaller than the ISS values found for the samples without defects. One can conclude that rather negligible effects on the ISS values have the defects with $A_{dp} \leq 2$ % (Figure 7).

Comparable numbers of defective samples n_{ds} were found in each of the investigated groups: Group A n_{ds} =14, Group B n_{ds} =14, Group C n_{ds} =15, Group D n_{ds}=13. This allows us to conclude that the generic combination irrigant/sealer did not have a direct influence on the defect generation process. Excluding the samples with defects, the interfacial shear strength on average increased by 30 % (Figures 6a and 6b), as well as the standard deviation averagely decreased by more than 25 % (Tables 2 and 3).

The results obtained in the present study lead us to conclude that future research guidelines should be focused on the development of innovative protocols that allow the number and the dimensions of the defects to be minimized.

Conclusions

The experimental results showed that the tested groups are equivalent and no statistically significant differences can be seen. Histomorphometric analyses revealed that, in spite of the attention paid by the operator, different defects were included in the samples and these led to a significant decrease of the ISS. Averagely, the interfacial shear strength found for the samples without defects was about twice as large as that found for the samples with defects. The defects occupying more than 12 % of the total transverse section area of the endodontic cement layer, led to interfacial shear strength values 70 % smaller than those found for the samples without defects. Those occupying less than 2 %, instead, had rather negligible effects on the interfacial shear strength.

Competing Interests

The authors have declared that no competing interest exists.

References

1. King PA, Setchell DJ. An in vitro evaluation of a prototype CFRC prefabricated post developed for the restoration of pulpless teeth. J Oral Rehabil. 1990; 17: 599-609.
2. Isidor F, Odman P, Brøndum K. Intermittent loading of teeth restored using prefabricated carbon fibre posts. Int J Prosthodont. 1996; 9: 131-6.
3. Asmussen E, Peutzfeldt A, Heitmann T. Stiffness, elastic limit, and strength of newer types of endodontics posts. J Dent. 1999; 27: 275-8.
4. Magne P, Belser UC. Porcelain versus composite inlays/onlays: effects of mechanical loads on stress distribution, adhesion, and crown flexure. Int J Periodontics Restorative Dent. 2003; 23: 543-55.
5. Barjau-Escribano A, Sancho-Bru JL, Forner-Navarro L, et al. Influence of prefabricated post material on restored teeth: fracture strength and stress distribution. Oper Dent., 2006; 31: 47-54.
6. Prisco D, De Santis R, Mollica F, et al. Fiber post adhesion to resin luting cements in the restoration of endodontically-treated teeth. Oper Dent. 2003; 28: 515-21.
7. Assif D, Gorfil C. Biomechanical considerations in restoring endodontically treated teeth. J Prosthet Dent. 1994; 71: 565-7.
8. Morgano SM. Restoration of pulpless teeth: application of traditional principles in present and future contexts. J Prosthet Dent. 1996; 75: 375-80.
9. Stockton LW. Factors affecting retention of post systems: a literature review. J Prosthet Dent. 1999; 81: 380-5.

10. Heydecke G, Butz F, Strub JR. Fracture strength and survival rate of endodontically treated maxillary incisors with approximal cavities after restoration with different post and core systems: an in-vitro study. J Dent. 2001; 29: 427-33.

11. Huysmans MC, van der Varst PG. Finite element analysis of quasistatic and fatigue failure of post and cores. J Dent. 1993; 21: 57-64.

12. Soares CJ, Santana FR, Castro CG, et al. Finite element analysis and bond strength of a glass post to intraradicular dentin: comparison between microtensile and push-out tests. Dent Mater. 2008; 24: 1405-11.

13. Sudsangiam S, van Noort R. Do dentin bond strength tests serve a useful purpose? J Adhes Dent. 1999; 1: 57-67.

14. Goracci C, Tavares AU, Fabianelli A, et al. The adhesion between fiber posts and root canal walls: comparison between microtensile and push-out bond strength measurements. Eur J Oral Sci. 2004; 112: 353-61.

15. Boschian Pest L, Cavalli G, Bertani P, et al. Adesive post-endodontic restorations with fiber posts: push-out tests and SEM observations. Dent Mater. 2002; 18: 596-602.

16. Giachetti L, Scaminaci Russo D, Baldini M, et al. Push-out strength of translucent fibre posts cemented using a dual-curing technique or a light-curing self-adhering material. Int Endod J. 2012; 45: 249-56.

17. Teixeira CS, Alfredo E, Thomé LH, et al. Adhesion of an endodontic sealer to dentin and gutta-percha: shear and push-out bond strength measurements and SEM analysis. J Appl Oral Sci. 2009; 17: 129-35.

18. Demiryürek EO, Külünk S, Saraç D, et al. Effect of different surface treatments on the push-out bond strength of fiber post to root canal dentin. Oral Surg Oral Med Oral Pathol Oral Radiol Endod. 2009; 108: 74-80.

19. Narene AVK, Shankar P, Indira R. Effect of Surface Treatments on Push-out Strength of Three Glass Fiber Posts: An in vitro Study. Indian Journal of Multidisciplinary Dentistry. 2011; **1**: 255-9.

20. Cheylan JM, Gonthier S, Degrange M. In vitro push-out strength of seven luting agents to dentin. Int J Prosthodont. 2002; 15: 365-70.

21. Babb BR, Loushine RJ, Bryan TE *et al*. Bonding of selfadhesive (self-etching) root canal sealers to radicular dentine. J Endod. 2009; 35: 578-82.

22. Hashem AA, Ghoneim AG, Lutfy RA, et al. The effect of different irrigating solutions on bond strength of two root canal-filling systems. J Endod. 2009; 35: 537-40.

23. Jainaen A, Palamara JE, Messer HH. Effect of dentinal tubules and res-in-based endodontic sealers on fracture properties of root dentin. Dent Mater. 2009; 25: 73-81.

24. Vilanova WV, Carvalho-Junior JR, Alfredo E. Effect of intracanal irrigants on the bond strength of epoxy resin-based and methacrylate res-in-based sealers to root canal walls. Int Endod J. 2012; 45: 42-8.

25. Akisue E, Tomita VS, Gavini G, et al. Effect of the combination of sodium hypochlorite and chlorhexidine on dentinal permeability and scanning electron microscopy precipitate observation. J Endod. 2010; 36: 847-50.

26. Wang CS, Arnold RR, Trope M, et al. Clinical efficiency of 2% chlorhexidine gel in reducing intracanal bacteria. J Endod. 2007; 33: 1283-9.

27. Jainaen A, Palamara JE, Messer HH. Push-out bond strengths of the dentine-sealer interface with a without a main cone. Int Endod J. 2007; 40: 882-90.

28. [Internet] CEMENTI COMPOSITI. http://www.mcitaliasrl.com/surgi_cem-dualflo.htm

29. Pegoretti A, Fambri L, Zappini G, et al. Finite element analysis of a glass fibre reinforced composite endodontic post. *Biomaterials*. 2002; 23: 2667-82.

30. Verhulp E, van Rietbergen B, Huiskes R. Comparison of micro-level and continuum-level voxel models of the proximal femur. J Biomech. 2006; 39: 2951-7.

31. Casavola C, Lamberti L, Pappalettere C, et al. A comprehensive numerical stress - Strain analysis of laser beam butt-welded titanium compared with austenitic steel joints. J Strain Anal Eng. 2010; 45: 535-54.